Mineralogical Magazine, December 2013, Vol. 77(8), pp. 3137–3153

Rinkite, cerianite-(Ce), and hingganite-(Ce) in syenite gneisses from the Sushina Hill Complex, India: occurrence, compositional data and petrogenetic significance

A. Chakrabarty[1,*], R. H. Mitchell[2], M. Ren[3], A. K. Sen[4] and K. L. Pruseth[4,5]

[1] Department of Geology, Durgapur Government College, Durgapur, West Bengal, 713214, India
[2] Department of Geology, Lakehead University, Thunder Bay, Ontario, Canada P7B 5E1
[3] Department of Geoscience, University of Nevada, Las Vegas, Nevada, USA
[4] Department of Earth Sciences, Indian Institute of Technology Roorkee, Roorkee, Uttarakhand-247667, India
[5] Department of Geology and Geophysics, Indian Institute of Technology Kharagpur, Kharagpur, 721302, India

[*Received 11 July 2013; Accepted 30 October 2013; Associate Editor: W. Crichton*]

ABSTRACT

Accessory rare earth element (*REE*) minerals occur in small quantities in agpaitic and miaskitic nepheline syenite gneisses of the Sushina Hill Complex, India. The *REE*-rich minerals restricted mainly to the agpaitic rocks are rinkite, cerianite-(Ce), and cerian thorite. Rinkite, formed at the ortho-magmatic stage predates other *REE*-rich phases and is the most Nd-F-rich rinkite (6.62–7.45 wt.% Nd_2O_3; 8.75–9.74 wt.% F) with very high Nd/Ce (>2.46) ratios reported to date. Hydrothermal cerianite-(Ce), formed by the decomposition of eudialyte in the agpaitic rocks, occurs as small rounded crystals rich in Ce (~63–74 wt.% CeO_2) and Y (6.03–11.69 wt.% Y_2O_3). The presence of cerianite-(Ce) indicates formation in an evolving hydrothermal fluid in an oxidizing milieu. Hingganite-(Ce) is present in the miaskitic unit and is considered to represent the superposition of an agpaitic mineral on an initial miaskitic assemblage. Hingganite-(Ce) is characterized by elevated contents of Ce (18.03–21.94 wt.% Ce_2O_3), and Nd (13.90–15.40 wt.% Nd_2O_3). Experimental data, coupled with the observed assemblage, suggest that the hingganite-(Ce) precipitated from the hydrothermal fluid between 400 and 300ºC followed by cerianite-(Ce) (<~300ºC). This conclusion implies that eudialyte decomposition was probably initiated above 400ºC.

Keywords: rinkite, cerianite-(Ce), hingganite-(Ce), eudialyte, agpaitic systems.

Introduction

Peralkaline nepheline syenites exhibit wide compositional variability which is expressed by the occurrence of exotic mineral assemblages. The term 'agpaitic' is given to peralkaline nepheline syenites. These rocks are characterized by: elevated contents of Na, Ca, K; high field strength elements (HFSE) such as Ti, Zr, Hf, Nb; rare earth elements (*REE*s); U and Th, together with Cl^- and F^-. The common typomorphic minerals of agpaitic nepheline syenites include eudialyte, rinkite, mosandrite, låvenite, aenigmatite, etc. In contrast, nepheline syenites, with a simpler mineralogy characterized by zircon, titanite (± ilmenite, magnetite), are termed "miaskitic" syenites (Sørensen, 1992, 1997). Agpaitic rocks, in general, are well known for hosting rare earth element mineralization of economic importance. Notable examples include: Ilímaussaq and Motzfeld (Greenland); Mont Saint Hilaire (Canada); Khibiny and Lovozero (Russia); Pilansberg (South Africa); Tamazeght (Morocco) (Mitchell and Liferovich,

* E-mail: aniket_chakrabarty@rediffmail.com
DOI: 10.1180/minmag.2013.077.8.08

2006; Pfaff *et al.*, 2008; Marks *et al.*, 2011; Schilling *et al.*, 2011). Rare examples of metamorphosed agpaitic syenites have been reported from the Red Wine (Canada) and Norra Kärr (Sweden) Complexes (Allan, 1992; Edgar and Blackburn, 1972; Adamson, 1944; Curtis and Currie, 1977; Blaxland, 1977).

Recently, an isolated occurrence of agpaitic nepheline syenite gneiss was described from the Sushina Hill Complex (22º57′N, 86º37′E) of West Bengal, India (Chakrabarty, 2009; Chakrabarty *et al.*, 2011, 2012; Mitchell and Chakrabarty, 2012). The complex is composed mainly of eudialyte nepheline syenite gneisses (agpaitic); nepheline syenite gneiss (miaskitic) and albitite (Chakrabarty *et al.*, 2013). In terms of composition, the eudialyte is extremely Mn-rich and similar to eudialyte found in Pilansberg lujavrites (Mitchell and Liferovich 2006, Chakrabarty *et al.*, 2012). Alteration of Mn-rich eudialyte leads to complex decomposition assemblages consisting of pectolite-serandite and diverse sodian-zirconosilicates such as hilairite, catapleiite/gaidonnayite. Rare earth elements-rich phases in these gneisses are represented mainly by rinkite, cerian thorite and ancylite (Mitchell and Chakrabarty, 2012). Miaskitic gneisses are relatively rare and constitute only a minor part of the Sushina Hill Complex (Chakrabarty *et al.*, 2013). The major *REE*-bearing species in these gneisses are zircon, titanite and hingganite-(Ce).

In this work, we describe new occurrences and compositional data for cerianite-(Ce); F-bearing rinkite-(Nd) in agpaitic rocks, and hingganite-(Ce) from miaskitic gneisses.

Geological setting

The Mesoproterozoic Sushina Hill complex (22º57′N, 86º37′E) (~480 m × 93 m) lies within Chandil Formation of North Singhbhum Mobile Belt, along a shear zone termed the Northern Shear Zone (Saha, 1994). This 100 km-long WNW−ESE trending discontinuous shear zone is located at the contact between the Chotanagpur Granitic Gneissic Complex in the north and the Chandil Formation in the south (Fig. 1*a*,*b*). The shear zone is believed to be an extension of the Central Indian Shear Zone (Rekha *et al.*, 2011). Alkaline intrusive rocks such as carbonatite, alkali-pyroxenite, and nepheline syenite occur along the Northern Shear Zone (Basu, 1993; Chakrabarty *et al.*, 2009, 2011, 2012; Mitchell and Chakrabarty, 2012; Chakrabarty and Sen, 2010, 2013). The Sushina Hill complex is composed of diverse undersaturated syenite gneisses together with country rocks consisting of sodic schists and amphibolites. Two varieties of nepheline syenite gneiss, eudialyte nepheline gneiss (agpaitic) and miaskitic nepheline gneiss, have been recognized at the Sushina Hill complex (Fig. 1*c*) (Chakrabarty, 2009).

Miaskitic nepheline syenite gneisses are relatively rare and represent only a minor part of the complex (Fig. 1*c*). These are composed of albite, orthoclase, nepheline, minor late-stage eastonitic biotite and accessory thorite, unidentified Mn-Fe oxides and hingganite-(Ce) (Chakrabarty *et al.*, 2013; Mitchell and Chakrabarty, 2012). The miaskitic mineral assemblage is defined by the presence of zircon and manganoan-magnetite. The miaskitic gneisses do not show any visible gneissosity in their surficial expression. However, granuloblastic, deformation and recrystallization textures demonstrate the metamorphosed character of this unit. The emplacement age of the miaskitic syenite is ~1.51 Ga and is considered to be the oldest unit of the complex (Chakrabarty, 2009; Chakrabarty *et al.*, 2013). A similar age of ~1.55 Ga is also considered as the emplacement age of the carbonatite and anorthosite situated at the western and eastern extremities along the Northern Shear Zone (Chakrabarty and Sen, 2013; Chatterjee *et al.*, 2008).

Agpaitic gneisses, are characterized by the presence of the typomorphic minerals eudialyte and rinkite. These occur together with albite, orthoclase, nepheline, aegirine, and arfvedsonite. This gneiss is characterized by layering resulting from variations in the modal proportions of nepheline, feldspar, and ferromagnesian minerals. The mafic minerals coalesce and cluster, giving rise to a gneissic texture as well as a ‘knotted’ or mottled appearance. The occurrence of metamorphic piemontite together with recrystallization textures between albite, orthoclase and nepheline is suggestive of a metamorphic overprint on the precursor eudialyte syenite (Chakrabarty, 2009; Goswami and Basu, 2013). The trend of the gneissic bands in the syenite gneisses is identical to that of the Northern Shear Zone, i.e. WNW−ESE. The crystallization age of the precursor nepheline syenite is not well constrained. A recent study of the post-magmatic eudialyte by Rb-Sr, Sm-Nd, and Lu-Hf methods confirms that eudialyte precipitation from the deuteric fluid occurred at 1.30 Ga and therefore the age of the host agpaitic syenite is considered

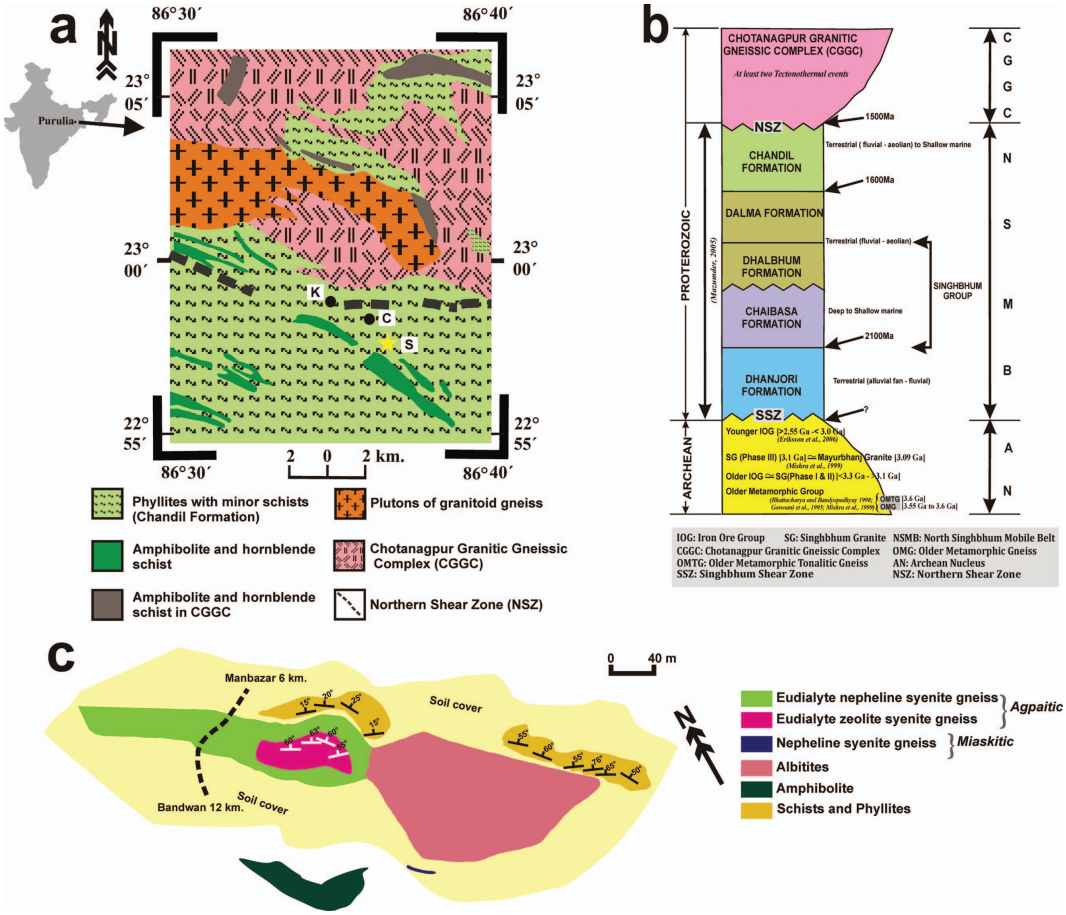

FIG. 1. (*a*) Regional geological map of part of the Purulia–Chotanagpur area along the Northern Shear Zone. The present study area is located at S (Sushina) and marked by a yellow star. K (Kutni) and C (Chirugora) are two important localities of alkaline magmatism, mainly carbonatite and apatite-magnetite within the mappable area. (*b*) Revised chronostratigraphic succession of the Singhbhum-Chotanagpur area. (*c*) Detailed lithological map of the Sushina Hill complex showing the dispositions of different litho units within the complex.

slightly older than this 1.30 Ga hydrothermal event (authors' unpublished data).

A large body of an albitite is juxtaposed with the gneisses and is not mineralogically well constrained. Preliminary studies show it is characterized by albite, orthoclase, chlorite, zircon, monazite, xenotime, magnetite and various unidentified Mn-Fe oxides.

It is now well established that the rocks of both the Chotanagpur Granitic Gneissic Complex and the North Singhbhum Mobile Belt experienced polyphase metamorphism accompanied by distinctive deformational events from ~1.87 to 0.78 Ga (Maji *et al.*, 2008; Sanyal and Sengupta, 2012; Rekha *et al.*, 2011). The earliest metamorphic event is recorded within the granulite enclaves in the Chotanagpur Granitic Gneissic Complex at ~1.87 Ga (>900ºC at ~5–8 kbar). This was followed by felsic magmatism and contemporaneous metamorphism at ~1.66–1.55 Ga. It is interesting that these older metamorphic events are not evident within the rocks of the Chandil Formation or in other parts of the North Singhbhum Mobile Belt. Alkaline magmatism (carbonatite and nepheline syenite) was accompanied by the intrusion of a suite of anorthosite and porphyritic granitoids at ~1.55–1.51 Ga. These experienced greenschist-

to-amphibolite-facies metamorphism (~700±50ºC, 0.65±0.1 GPa) between 1.20 and 0.93 Ga. A final phase of metamorphism (600−750ºC at 0.7±0.1 GPa) is related mainly to de-fragmentation of the Rodinia supercontinent which affected the entire eastern margin of the Indian subcontinent at ~0.87−0.78 Ga and resulted in the formation of the Eastern Indian Tectonic Zone (Chatterjee *et al.*, 2010). This last metamorphic event is widespread both within the Chotanagpur Granitic Gneissic Complex and the North Singhbhum Mobile Belt (Chatterjee and Ghosh, 2011; Rekha *et al.*, 2011). Although the detailed metamorphic history of the Sushina Hill Complex is yet to be investigated systematically, available data suggest that the rocks of the Sushina Hill Complex experienced metamorphism at ~1.20 and 0.87 Ga, respectively (Chakrabarty, 2009; Chakrabarty and Sen, 2013).

Analytical methods

The *REE*-bearing minerals were analysed in polished thin sections using a JXA-8900 Super Probe and CAMECA SX-100 electron microprobes at the EMIL (Electron Microanalysis and Imaging Laboratory), University of Nevada, Las Vegas (UNLV), USA and IIC (Institute Instrumentation Centre), Indian Institute of Technology Roorkee, India. Polished sections were examined by optical microscopy to identify target areas for analysis prior to EMP data collection. Selection of analytical sites was guided by backscattered electron imagery. The instruments operated in wavelength dispersive (WD) mode equipped with four WD spectrometers and one energy dispersive (ED) spectrometer. The samples were analysed using LLIF, LPET and standard PET crystals (CAMECA SX-100) at IIC under the following conditions: 15 kV accelerating voltage, 20 nA beam current and 1−3 μm beam diameter. As standards, we used pure synthetic *REE* phosphates (*REEL*α for La, Ce, Yb, Lu; *REEL*β for the remaining *REE*s), YPO_4 (Y*L*α), UO_2 (U*M*β), ThO_2 (Th*M*α), fayalite (Fe*K*α), wollastonite (Si*K*α, Ca*K*α), olivine (Mg*K*α), sanidine (Al*K*α), zircon (Zr*L*α), titanite (Ti*K*α), Nb (Nb*L*α), Al_2O_3 (Al*K*α), rhodonite (Mn*K*α), albite (Na*K*α) and BaF_2 (F*K*α).

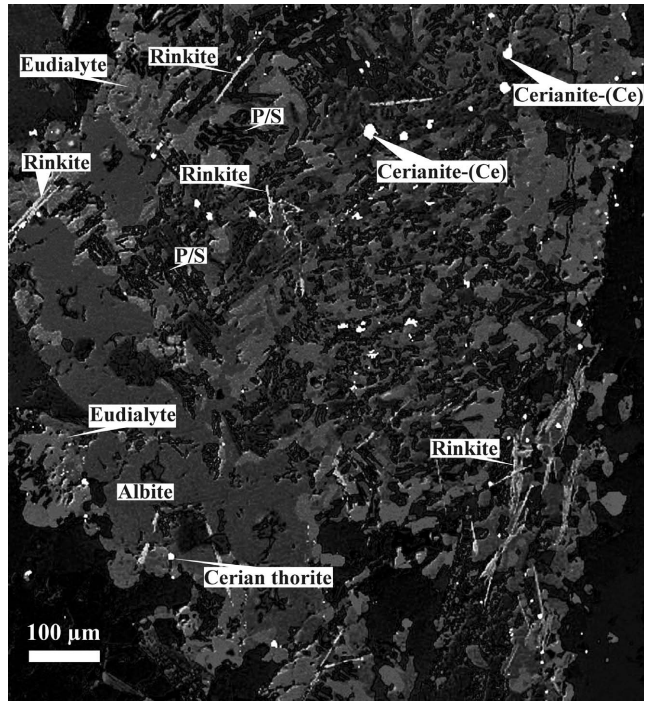

FIG. 2. Back-scattered electron image showing randomly oriented, elongate, needle-shaped rinkite crystals embedded within the albite and eudialyte, and its decomposition assemblage represented by pectolite-serandite (P/S) in agpaitic gneiss. Note the presence of dispersed grains of cerianite and cerian thorite close to the rinkite.

Special attention was given to ensuring that line overlaps were properly corrected and that background interference was avoided. Empirically determined correction factors applied to the following line overlaps were: Th→U, Dy→Eu, Gd→Ho, La→Gd, Ce→Gd, Eu→Er, Gd→Er, Sm→Tm, Dy→Lu, Ho→Lu and Yb→Lu (Pršek *et al.*, 2010). Each peak was measured for 30 or 50 s (10 and 25 s for the background, respectively). Matrix corrections used a ZAF correction program package on the JEOL 8900 and the PAP method for the CAMECA EMP, respectively (Pouchou and Pichoir, 1991). In all analyses, alkali elements Na and K were counted on the first WDS cycle to minimize potential element migration caused by beam damage. Analytical precision on the basis of replicate analyses of standards has standard deviation of <0.5% for major and <0.1% for minor elements.

Paragenesis and compositions

Rinkite

Rinkite, ideally $Na_2Ca_4REETi(Si_2O_7)_2OF_3$ (Cámara *et al.*, 2011) occurs as long needle-like prismatic crystals embedded in albite and also within the eudialyte alteration assemblage (Figs 2, 3) in agpaitic gneiss. Individual rinkite crystals are 5–10 μm long and typically associated with the alteration assemblage of pectolite-serandite and hilairite formed after eudialyte (Fig. 2) (Mitchell and Chakrabarty, 2012). Rarely, elongated rinkite crystals are found to be embedded within albite without any eudialyte alteration assemblages. Growing eudialyte crystals are terminated against such rinkite crystals (Fig. 3). Consequently, rinkite is considered as a relict primary phase. Rinkite is *MREE*-rich, particularly in Nd (Fig. 4), with Nd/Ce ratios >2.46 and characterized by very high F contents (⩾3.75 a.p.f.u.) (Table 1). Nd enrichment in the rinkite investigated was reported previously by Mitchell and Chakrabarty (2012) (Nd/Ce >1.42). Such Nd- and F-rich rinkite (6.62–7.45 wt.% Nd_2O_3; 0.32–0.35 a.p.f.u.; 8.75–9.74 wt.% F; 3.75–4.03 a.p.f.u.) has not been described previously from other localities. The limited number of published compositional data for rinkite gave Nd and F contents of 1.89–4.91 wt.% Nd_2O_3 (0.09–0.24 a.p.f.u.) and 5.82–7.48 wt.% (2.47–3.20 a.p.f.u.), respectively (Cámara *et al.*, 2011; Lorenzen, 1884). Thus, our data represent the most Nd-, F-rich rinkite reported to date.

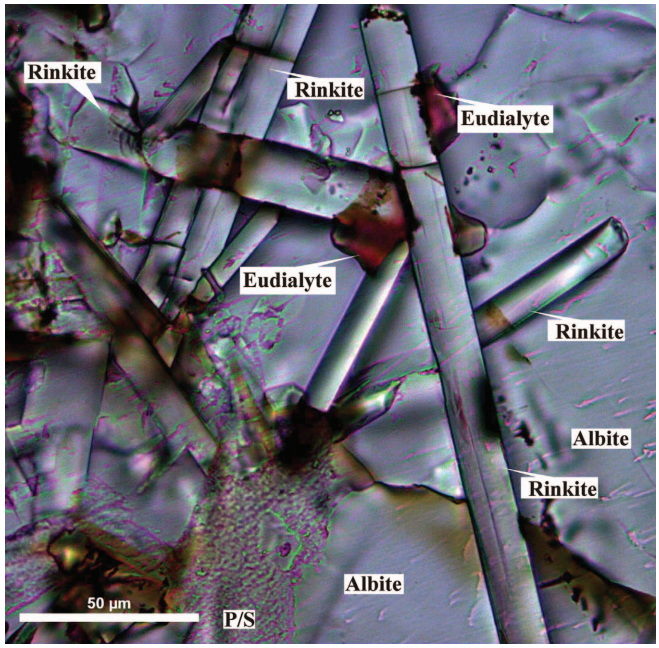

FIG. 3. Rare occurrence of a long, prismatic rinkite crystal embedded in albite without a eudialyte alteration assemblage. Small eudialyte crystals terminate against the early-formed rinkite crystals.

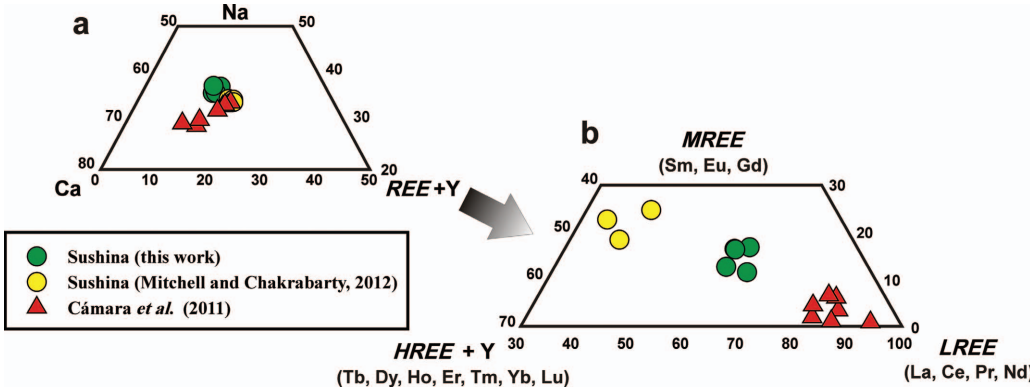

FIG. 4. (*a*) Ternary diagram showing compositional variation in terms of Ca-(*REE*+Y)-Na (a.p.f.u.) for rinkite. Note that the investigated rinkite is relatively enriched in Na compared to other reported occurrences. (*b*) Ternary diagram showing variation in *REE* (a.p.f.u.) of rinkite. Compared to other reported occurrences, the rinkite is relatively rich in light−middle rare earth elements (*LREE*−*MREE*) and poorer in heavy rare earth elements (*HREE*) and Y.

TABLE 1. Representative compositions of rinkite.

Wt.%	1	2	3	4	5
P_2O_5	n.d.	n.d.	n.d.	n.d.	n.d.
Nb_2O_5	2.39	2.03	1.68	1.93	1.36
Ta_2O_5	n.d.	n.d.	n.d.	n.d.	n.d.
SiO_2	28.85	29.45	30.73	29.76	30.60
TiO_2	7.95	8.00	7.86	7.87	8.06
ZrO_2	0.00	0.18	0.99	0.58	1.25
ThO_2	n.d.	n.d.	n.d.	n.d.	n.d.
Al_2O_3	0.00	0.01	0.00	0.16	0.10
Y_2O_3	1.78	1.71	1.89	1.99	1.89
La_2O_3	1.38	1.56	1.03	1.02	1.06
Ce_2O_3	2.10	2.20	2.39	2.74	1.37
Pr_2O_3	1.02	0.89	1.75	0.92	0.65
Nd_2O_3	7.16	6.92	7.27	6.62	7.45
Sm_2O_3	1.32	1.35	1.31	1.34	1.31
Eu_2O_3	0.00	0.00	0.00	0.00	0.00
Gd_2O_3	2.01	2.03	1.05	1.92	1.03
Dy_2O_3	1.10	1.98	1.71	1.38	1.87
Er_2O_3	n.d.	n.d.	n.d.	n.d.	n.d.
Yb_2O_3	n.d.	n.d.	n.d.	n.d.	n.d.
FeO	0.07	0.13	0.03	0.04	0.00
MnO	0.12	0.04	0.11	0.16	0.62
MgO	0.00	0.00	0.07	0.00	0.03
CaO	24.95	25.41	23.29	23.77	24.01
SrO	0.41	0.61	0.67	0.54	0.94
BaO	n.d.	n.d.	n.d.	n.d.	n.d.
PbO	n.d.	n.d.	n.d.	n.d.	n.d.
Na_2O	9.72	10.23	9.81	9.38	9.91
K_2O	0.01	0.00	0.00	0.00	0.05
F	8.75	8.96	8.92	9.44	9.74
Cl	0.00	0.00	0.00	0.00	0.00
Total	101.10	103.70	102.56	101.57	103.29
O=F	3.69	3.77	3.76	3.97	4.10
Total	97.41	99.93	98.80	97.59	99.19

Table 1 (*contd.*)

Wt.%	1	2	3	4	5
Structural formulae (O = 18)					
Ta	0.00	0.00	0.00	0.00	0.00
Nb	0.15	0.12	0.10	0.12	0.08
Ti	0.81	0.80	0.79	0.79	0.79
Zr	0.00	0.01	0.06	0.04	0.08
Al	0.00	0.00	0.00	0.02	0.02
$\Sigma M^{O}(1)$	0.96	0.93	0.95	0.97	0.97
Si	3.91	3.91	4.08	3.99	4.01
La	0.07	0.08	0.05	0.05	0.05
Ce^{3+}	0.10	0.11	0.12	0.13	0.07
Pr	0.05	0.04	0.08	0.04	0.03
Nd	0.35	0.33	0.34	0.32	0.35
Sm	0.06	0.06	0.06	0.06	0.06
Eu	0.00	0.00	0.00	0.00	0.00
Gd	0.09	0.09	0.05	0.09	0.04
Dy	0.05	0.08	0.07	0.06	0.08
Er	0.00	0.00	0.00	0.00	0.00
Yb	0.00	0.00	0.00	0.00	0.00
Th	0.00	0.00	0.00	0.00	0.00
Y	0.13	0.12	0.13	0.14	0.13
ΣREE	0.90	0.91	0.91	0.89	0.81
Ca	3.07	3.04	3.04	3.06	3.12
Ba	0.00	0.00	0.00	0.00	0.00
Sr	0.03	0.05	0.05	0.04	0.07
ΣM^{2+}	3.10	3.09	3.09	3.10	3.19
Fe^{2+}	0.01	0.01	0.00	0.00	0.00
Mn^{2+}	0.01	0.00	0.01	0.02	0.07
Mg	0.00	0.00	0.01	0.00	0.01
Ca	0.56	0.58	0.27	0.35	0.25
Na	2.56	2.63	2.52	2.44	2.52
K	0.00	0.00	0.00	0.00	0.01
$\Sigma M^{O}(2)+2M^{O}(3)$	3.14	3.23	2.82	2.81	2.85
$\Sigma 2M^{H}+2A^{P}$	4.00	4.00	4.00	4.00	4.00
ΣCations	12.01	12.08	11.85	11.77	11.83
F	3.75	3.76	3.75	4.00	4.03

Cerianite-(Ce)

Cerianite-(Ce), ideally CeO_2, was initially described from a xenolith in a carbonatite dyke at Lackner Lake, Ontario, Canada (Graham, 1955). Cerianite-(Ce) occurs at many localities worldwide principally as a secondary phase (see Table 2). Compositional data for cerianite-(Ce) are limited except for the recent study of Zaitsev *et al.* (2011).

In common with rinkite, cerianite-(Ce) in the agpaitic gneisses is present in association with the alteration assemblages formed after eudialyte. Small rounded grains of cerianite-(Ce), usually 5−7 μm in diameter, are scattered throughout the alteration assemblage composed of hilairite and pectolite-serandite (Fig. 5). Small rounded crystals of cerian thorite are also present in association with the cerianite-(Ce) (Mitchell and Chakrabarty, 2012). Cerianite-(Ce) is strongly enriched in light rare earth elements (*LREE*s) (70.55−78.96 wt.% and 0.80−0.86 a.p.f.u., respectively), and Y (6.03−11.69 wt.% Y_2O_3 and 0.05−0.11 a.p.f.u., respectively) (Fig. 6; Table 3). One Th-rich grain (7.07 wt.% ThO_2, Table 3, composition 10) of cerianite-(Ce) is completely devoid of Y, and is considered as Th-bearing cerianite. Compared to

TABLE 2. Important occurrences of the cerianite and gadolinite groups of minerals.

Lithology (host rock)	Locality
[I] Phonolites and nepheline syenites (weathered)	Morro do Ferro, Brazil[1]
[I] Hydrothermal vein of carbonatitic origin (?)	Karonge, Burundi[2]
[I] Granitic pegmatite	Nesöya, East Antarctica[3]
[I] Alluvial deposits (alteration product of fluocerite)	Afu Hills, Nigeria[4]
[I] Carbonatites (weathered)	Mount Weld, Australia[5]
[I] Syenite (weathered)	Akongo, Cameroon[6]
[I] Palaeosols	Flin Flon, Canada[7]
[I]Carbonate rocks	Lackner Township, Sudbury, Canada[8]
[I, II] Bastnäs deposit (alteration product of fluocerite)	South central Sweden[9]
[I] Alkaline pegmatites	Mount Malosa, Malawi[10]
[I] Metasomatic rocks	Terskii greenstone belt, Kola, Russia[11]
[I] Carbonatitic rocks, Kerimasi volcano	Gregory Rift, Tanzania[12]
[II] Syenite pegmatite	Skien, Norway[13]
[II] Granitic pegmatite and aplite	Strange Lake Peralkaline complex, Quebec-Labrador, Canada[14]
[II] Mariolitic granite and leucogranite	Baveno and Cuasso al Monte, Alps, Italy[15]
[II] Magnetite deposit	Bacúch, Slovakia[16]
[II]A-type granite	Wentworth Pluton, Nova Scotia, Canada[17]

I: Cerianite and II: Gadolinite.
1. Frondel and Marvin (1959); 2. Van Wambeke (1977); 3. Matsumoto and Sakamoto (1982); 4. Styles and Young (1983); 5. Lottermoser (1987); 6. Braun *et al.* (1990); 7. Pan and Stauffer (2000); 8. Graham (1955); 9. Holtstam and Andersson (2007); 10. Guastoni *et al.* (2009); 11. Skublov *et al.* (2009); 12. Zaitsev *et al.* (2011); 13. Segalstad and Larsen (1978); 14. Jambor *et al.* (1998); 15. Pezzotta *et al.* (1999); 16. Pršek *et al.* (2010); 17. Papoutsa and Pe-Piper (2013).

other cerianite-(Ce) occurrences, Suhsina cerianite-(Ce) is characterized by the presence of Nb (0.44–1.16 wt.% Nb_2O_5) and Zr (0.99–1.89 wt.% ZrO_2) and traces of Ca, Mn, Ti, Na and Si (Table 3). Characteristically, the cerianite-(Ce) is rich in CeO_2 (~63–74 wt.% and 0.75–0.84 a.p.f.u., respectively) and comparable to that from Bastnäs (Sweden) and Lackner Lake (Canada), whereas Kisete (Tanzania) cerianite-(Ce) is exceptionally rich in Y and Nd (Fig. 6). Bastnäs and Kisete cerianite-(Ce) is also characterized by elevated F contents ranging between 0.98 and 3.46 wt.% (Holtstam and Andersson, 2007; Zaitsev *et al.*, 2011). Thus, the Sushina cerianite-(Ce) is the second most yttrium and lanthanide-rich cerianite-(Ce) known after the Kisete occurrence. However, it must be noted that Belkin *et al.* (2009) reported interference between F$K\alpha$ (λ = 18.3199 Å) and Ce$M\zeta$ (λ = 18.3499 Å) when Ce_2O_3 > 10% wt.% for the chevkinite-group minerals. Given the very high CeO_2 content in the cerianite-(Ce) analysed, we note that determination of the F content should be undertaken by other methods.

Hingganite

Minerals of the gadolinite–datolite group have been reported from both silica-saturated and silica-undersaturated rocks worldwide (see Table 2). There exist nine IMA-approved members in this group and the compositional variability among the members of the gadolinite group arise mainly due to variation in the content of Y, Ce, Ca, Fe and Yb together with Be, B and OH (Demartin *et al.*, 2001; Grew, 2002). Recently, an Nd-dominant hingganite was recognized by Pršek *et al.* (2010) from the Bacúch magnetite deposits of Slovakia.

Hingganite-(Ce) was found in a single sample of miaskitic gneiss. Most hingganite-(Ce) grains are anhedral (~0.07–0.10 mm × 0.04 mm) and intimately associated with zircon (Fig. 7). However, smaller (~3 μm) isolated euhedral crystals are also present (Fig. 7*a*). Textural relationships suggest that the hingganite is hydrothermal in origin as it is commonly found replacing the magmatic zircons (Fig. 7*b*).

It is difficult to characterize the gadolinite group of minerals by EPMA data alone. X-ray

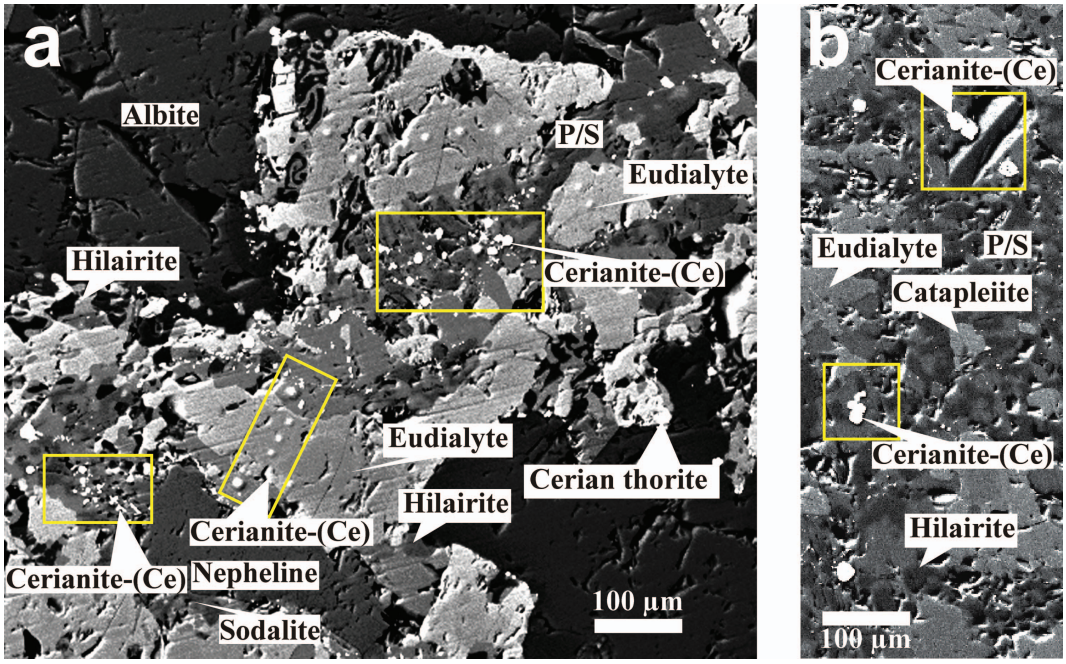

FIG. 5. (*a*) Small, anhedral, rounded grains (bright spots) of cerianite-(Ce) scattered throughout the decomposition assemblage formed after eudialyte. The majority of the cerianite-(Ce) grains are restricted to the pectolite-serandite alteration assemblage. (*b*) Cerianite-(Ce) associated with the sodic zirconosilicates represented by the catapleiite and hilairite. Concentrations of cerianite-(Ce) grains are outlined by the yellow boxes.

diffraction analysis of a single crystal was carried out using a Philips X'Pert Pro (PW3040/60) instrument with Ni-filtered Cu$K\alpha$ radiation for identification of the transparent crystals associated with the zircons. The XRD data were recorded at 40 kV and 30 mA by counting at 0.5 s intervals, at steps of 0.05º2θ, from 20 to 80º2θ. Dimensions of the unit cell were calculated using

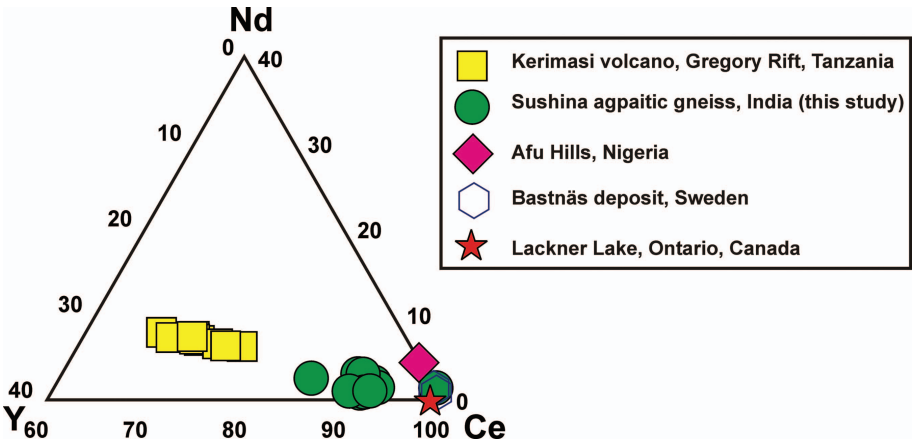

FIG. 6. Ternary diagram showing compositional variation in terms of Ce, Nd and Y (a.p.f.u.) in cerianite-(Ce) from Sushina and other localities. Sources of data are given in Table 2.

TABLE 3. Representative compositions of cerianite-(Ce).

Wt.%	1	2	3	4	5	6	7	8	9	10
Nb_2O_5	1.07	1.08	1.59	1.36	2.15	0.80	0.44	0.80	1.25	1.16
SiO_2	0.83	1.20	1.05	0.92	1.82	0.32	0.67	0.32	1.01	1.96
ThO_2	0.00	0.00	0.00	0.00	0.00	0.00	0.00	0.00	0.00	7.07
ZrO_2	1.09	0.99	0.99	1.43	1.16	1.56	1.36	1.56	1.43	1.89
TiO_2	0.19	0.37	0.18	0.26	0.35	0.23	0.12	0.23	0.25	0.24
CeO_2	63.35	68.24	72.54	72.34	69.58	71.65	73.94	71.65	71.32	68.93
La_2O_3	2.21	2.19	2.07	1.12	2.17	2.73	0.08	2.23	2.13	2.27
Pr_2O_3	1.35	1.32	1.15	1.46	0.00	0.00	0.00	0.00	0.00	0.13
Nd_2O_3	3.64	4.48	3.10	2.16	1.15	4.58	1.41	1.58	1.56	1.88
Sm_2O_3	1.36	1.61	1.23	1.10	1.68	1.29	1.21	1.34	1.42	1.53
Eu_2O_3	0.00	0.52	0.00	0.51	0.00	0.53	0.47	0.00	0.00	0.00
Gd_2O_3	1.89	1.25	0.92	1.28	1.56	1.51	1.76	1.32	1.35	2.19
Tb_2O_3	0.28	0.31	0.05	0.33	0.37	0.32	0.33	0.04	0.32	0.05
Dy_2O_3	1.57	2.10	1.04	2.02	2.12	1.32	2.17	2.28	2.51	2.01
Ho_2O_3	0.22	0.30	0.31	0.33	0.32	0.33	0.30	0.44	0.38	0.31
Er_2O_3	1.52	1.37	0.99	1.43	0.99	1.45	1.51	1.51	1.67	1.49
Tm_2O_3	0.33	0.35	0.37	0.35	0.33	0.37	0.35	0.40	0.42	0.50
Yb_2O_3	1.75	1.41	1.32	1.32	1.36	1.35	1.48	1.34	1.38	1.15
Lu_2O_3	0.61	0.55	0.66	0.61	0.66	0.61	0.66	0.65	0.51	0.60
Y_2O_3	11.69	7.01	6.13	6.03	7.97	6.81	7.91	9.32	6.94	0.00
Al_2O_3	0.13	0.19	0.97	0.00	0.00	0.00	0.00	0.00	0.04	0.01
MnO	0.18	0.16	0.17	0.92	1.20	0.35	0.11	0.35	0.84	0.41
CaO	0.28	0.24	0.48	0.75	0.92	0.32	0.20	0.32	0.69	0.44
Na_2O	0.13	0.18	0.51	0.12	0.35	0.04	0.00	0.04	0.26	0.45
Total	97.72	97.68	98.11	98.15	98.21	98.47	96.49	97.72	97.68	98.11
Structural formulae based on total cations = 1										
Nb	0.008	0.008	0.011	0.010	0.015	0.006	0.003	0.006	0.009	0.009
Si	0.014	0.020	0.017	0.015	0.029	0.005	0.011	0.005	0.016	0.033
Th	0.000	0.000	0.000	0.000	0.000	0.000	0.000	0.000	0.000	0.027
Zr	0.009	0.008	0.008	0.011	0.009	0.012	0.011	0.012	0.011	0.015
Ti	0.002	0.005	0.002	0.003	0.004	0.003	0.001	0.003	0.003	0.003
Ce	0.750	0.783	0.796	0.806	0.767	0.813	0.838	0.811	0.797	0.805
La	0.014	0.013	0.012	0.007	0.013	0.016	0.000	0.013	0.013	0.014
Pr	0.008	0.008	0.007	0.008	0.000	0.000	0.000	0.000	0.000	0.001
Nd	0.022	0.026	0.017	0.012	0.006	0.027	0.008	0.009	0.009	0.011
Sm	0.008	0.009	0.007	0.006	0.009	0.007	0.007	0.007	0.008	0.009
Eu	0.000	0.003	0.000	0.003	0.000	0.003	0.003	0.000	0.000	0.000
Gd	0.011	0.007	0.005	0.007	0.008	0.008	0.009	0.007	0.007	0.012
Tb	0.002	0.002	0.000	0.002	0.002	0.002	0.002	0.000	0.002	0.000
Dy	0.009	0.011	0.005	0.010	0.011	0.007	0.011	0.012	0.013	0.011
Ho	0.001	0.002	0.002	0.002	0.002	0.002	0.002	0.002	0.002	0.002
Er	0.008	0.007	0.005	0.007	0.005	0.007	0.008	0.008	0.008	0.008
Tm	0.002	0.002	0.002	0.002	0.002	0.002	0.002	0.002	0.002	0.003
Yb	0.009	0.007	0.006	0.006	0.007	0.007	0.007	0.007	0.007	0.006
Lu	0.003	0.003	0.003	0.003	0.003	0.003	0.003	0.003	0.002	0.003
Y	0.106	0.061	0.051	0.051	0.067	0.059	0.068	0.080	0.059	0.000
Al	0.003	0.004	0.018	0.000	0.000	0.000	0.000	0.000	0.001	0.000
Mn	0.003	0.002	0.002	0.012	0.016	0.005	0.002	0.005	0.011	0.006
Ca	0.005	0.004	0.008	0.013	0.016	0.005	0.004	0.005	0.012	0.008
Na	0.004	0.006	0.016	0.004	0.011	0.001	0.000	0.001	0.008	0.015
Total	1.000	1.000	1.000	1.000	1.000	1.000	1.000	1.000	1.000	1.000

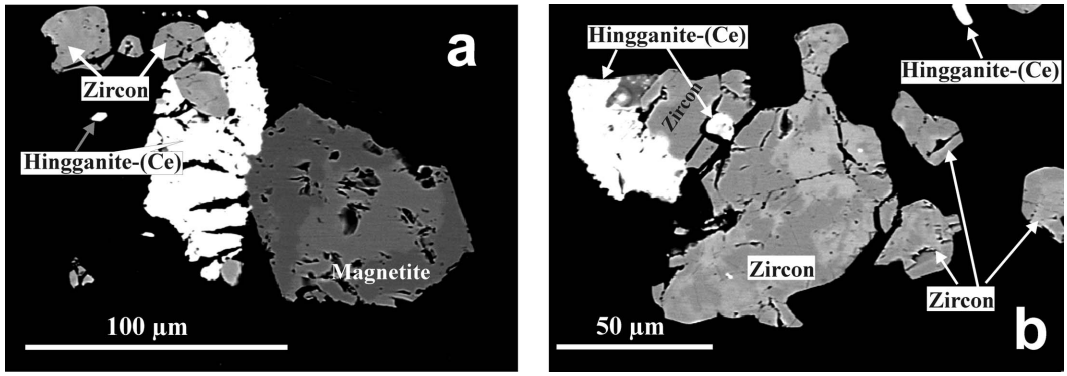

FIG. 7. (*a*) Large anhedral hingganite-(Ce) in association with zircons and magnetite in miaskitic gneiss. Note smaller euhedral crystals of hingganite-(Ce) present in isolation set within the albite matrix. (*b*) Hingganite-(Ce) replacing magmatic zircon in miaskitic gneiss. Such textural features indicate hydrothermal derivation of hingganite.

a least-squares refinement method. The unit-cell parameters of this sample (approximately a = 9.88, b =7.63, c = 4.75 Å, β = 90.42 and V = 357.98 Å^3) is nearly identical to the reported cell parameters of gadolinite-group minerals, especially hingganite-(Ce) (Ito and Hafner, 1974; Miyawaki *et al.*, 1984, 2007). Minerals of the gadolinite–datolite group at Sushina are represented exclusively by hingganite-(Ce), $Ce_2\square Be_2(Si_2O_8)(OH)_2$. Classification of gadolinite-group minerals is usually done on the basis of $^X\square/^X(\square+Fe^{2+})$ [$\square$: X-site vacancy] *vs.* W site (*REE*+Y)/(*REE*+Y+Ca) (Pršek *et al.*, 2010). Hingganite-(Ce) is generally Ca poor (~0.06 a.p.f.u.) but rich in *REE*s particularly in Ce, Nd and La (Table 4). The $^X\square/^X(\square+Fe^{2+})$ ratio ranges from 0.59 to 0.60 and Fe^{2+} reaches 0.41 a.p.f.u. (Table 4, Fig. 8*a*). All the analysed hingganite compositions exhibit a predominance of Ce over other *REE*s and Y (Ce/Y: 2.59−5.18) (Fig. 8*b*). However, a gadolinite-(Ce), $Ce_2Be_2FeSi_2O_8O_2$, component is probable as is

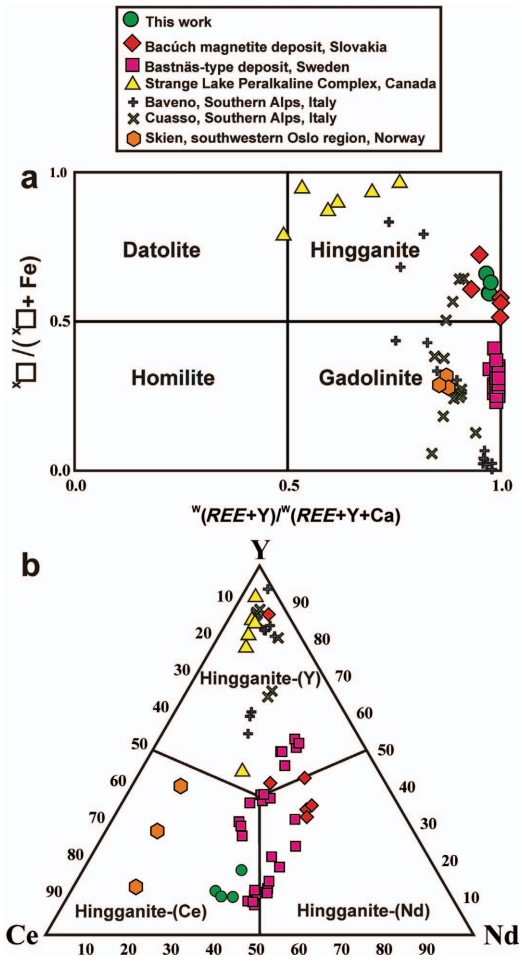

FIG. 8 (*right*). (*a*) Plot of compositions of minerals in the gadolinite–datolite group in terms of $^W(REE+Y)/^W(REE+Y+Ca)$ and $^X\square/^X(\square+Fe^{2+})$ showing that the mineral from Sushina is hingganite which is compositionally similar to hingganite reported from the Cuasso al Monte (Italy) and Bacúch magnetite deposit (Slovakia). (*b*) Triangular Y−Ce−Nd plot showing the occupancy at the W site in hingganite. The mineral from the miaskitic unit at Sushina is hingganite-(Ce). Sources of data on minerals from other localities are given in Table 2.

TABLE 4. Representative compositions of hingganite-(Ce).

Wt.%	1	2	3	4
SiO_2	23.40	22.89	23.13	23.32
La_2O_3	7.00	6.45	6.13	5.66
Ce_2O_3	21.94	21.52	19.95	18.03
Pr_2O_3	3.97	3.93	3.63	4.14
Nd_2O_3	13.90	14.63	15.40	14.98
Sm_2O_3	2.43	2.64	2.76	2.81
Eu_2O_3	0.00	0.00	0.00	0.00
Gd_2O_3	4.25	4.21	4.52	4.43
Tb_2O_3	0.33	0.37	0.34	0.38
Dy_2O_3	2.05	2.03	2.17	2.24
Ho_2O_3	0.17	0.56	0.87	0.98
Er_2O_3	0.00	0.00	0.00	0.00
Tm_2O_3	0.00	0.00	0.00	0.00
Yb_2O_3	0.00	0.00	0.00	0.00
Lu_2O_3	0.00	0.00	0.00	0.00
Y_2O_3	3.29	2.86	2.75	4.78
Al_2O_3	n.d.	n.d.	n.d.	n.d.
FeO	4.75	5.54	5.62	5.15
MnO	1.00	1.21	1.05	1.06
CaO	0.72	0.59	0.55	0.49
BeO*	9.74	9.53	9.63	9.71
Na_2O	n.d.	n.d.	n.d.	n.d.
Total	98.94	98.96	98.50	98.16
Structural formulae based on (Si+Al+P+S+As) = 2 and Be = 2 a.p.f.u.				
Si	2.000	2.000	2.000	2.000
La	0.221	0.208	0.195	0.179
Ce	0.686	0.688	0.632	0.566
Pr	0.124	0.125	0.114	0.129
Nd	0.424	0.456	0.476	0.459
Sm	0.072	0.079	0.082	0.083
Eu	0.000	0.000	0.000	0.000
Gd	0.120	0.122	0.130	0.126
Tb	0.009	0.011	0.010	0.011
Dy	0.056	0.057	0.060	0.062
Ho	0.005	0.016	0.024	0.027
Er	0.000	0.000	0.000	0.000
Tm	0.000	0.000	0.000	0.000
Yb	0.000	0.000	0.000	0.000
Lu	0.000	0.000	0.000	0.000
Y	0.150	0.133	0.127	0.218
Al	n.d.	n.d.	n.d.	n.d.
Fe	0.340	0.405	0.406	0.369
Mn	0.072	0.090	0.077	0.077
Ca	0.066	0.055	0.051	0.045
Be	2.000	2.000	2.000	2.000
Na	n.d.	n.d.	n.d.	n.d.
ΣT (Si+Al)*	2.000	2.000	2.000	2.000
ΣBe**	2.000	2.000	2.000	2.000
Fe^{2+}	0.340	0.405	0.406	0.369
$^{X}\square$	0.660	0.595	0.594	0.631
Σ*W* (*REE*+Y+Ca+Mn)	2.005	2.040	1.977	1.982
(*REE*+Y)/(*REE*+Y+Ca)	0.966	0.972	0.973	0.976
$^{X}\square/^{X}(\square + Fe^{2+})$	0.660	0.595	0.594	0.631

* The formulae calculation is based on Si = 2 a.p.f.u. as Al, P, S and As are below detection limits.
** Be calculated from ideal stoichiometry ($Be^{2+}+B^{3+}$ = 2 a.p.f.u.).

suggested by the significant amounts of Fe and Ce in all our data. The Ca-poor nature of the hingganite-(Ce) suggests that the datolite, $Ca_2B_2[Si_2O_8](OH)_2$, and homilite, $Ca_2FeB_2(Si_2O_8)$, components are either absent or minor, in contrast to the other reported occurrences such as in alpine fissures (Demartin *et al.*, 1993) and granitic pegmatites of Italy (Pezzotta *et al.*, 1999; Demartin *et al.*, 2001). The structural formula calculations give the sum of *REE*+Y+Ca as 1.90−1.95 a.p.f.u. Such deviations from the ideal 2 a.p.f.u. also reflect the partial vacancies in the crystal structure which are common for all hingganite species.

Discussion

Mitchell and Chakrabarty (2012) have described the mineralogy of the agpaitic gneisses of the Sushina Hill Complex and demonstrated the presence two varieties of Fe-Mn-poor eudialyte which differ significantly in their *REE* contents. Both types are altered, the alteration assemblage being represented by hilairite, catapleiite, etc. and pectolite–serandite. Mitchell and Chakrabarty (2012) suggested that the fluid responsible for eudialyte alteration was a deuteric fluid. The majority of the *REE*-bearing species at Sushina are restricted to the agpaitic gneisses, and specifically to the late-to-post-magmatic assemblages. Textural features indicate that rinkite is the earliest *REE*-bearing phase and predates eudialyte and related alteration assemblages as it is included in the eudialyte (Fig. 2). Rinkite, a Na-Ca-Ti-bearing silico-fluoride is a typomorphic mineral of agpaitic systems. Experimental data suggest a general affinity of *REE* for F, thus leading to the formation of stable fluoride complexes (Williams-Jones *et al.*, 2012; Pearson, 1963). Rinkite formation at the early stage of the crystallization history is evident as agpaitic magmas are generally enriched in the halogens (F^-, Cl^-). The paucity of *REE*s in late magmatic eudialyte is also explained by the fact that the majority of *REE*s are incorporated in the rinkite. Thus, the presence of rinkite indicates relative high alkalinity and an elevated Na/F ratio of the parent melt from which they crystallized during the early stage of the crystallization history, and in accord with the earlier observations of Mitchell and Chakrabarty (2012). In contrast to the available data reported in the literature, the rinkite investigated here is one of the most Nd-rich rinkites reported to date, with Nd/Ce > 2.36.

After rinkite formation, eudialyte began to crystallize. The significant Mn content of this eudialyte indicates that it is essentially late-to-post magmatic in origin. Eudialyte crystallization marks an increase in Cl^- activity (and Na/Cl ratio) of the evolving fluid and reaches a maximum during hydrothermal eudialyte precipitation from the deuteric fluids. It has been estimated that the crystallization temperature of the host agpaitic gneisses ranged between 500 and 600ºC (Chakrabarty, 2009; Mitchell and Chakrabarty, 2012), and thus eudialyte decomposition certainly took place below this temperature range and in accordance with the available experimental data. These experimental data show that eudialyte decomposition can take place under alkaline conditions at pH > 8, Na/Cl > 1 at 350ºC, 0.1 GPa (Markl and Baumgartner, 2002). During such decomposition, elements such as the *REE*, which cannot be accommodated in either the sodian-zirconosilicates or pectolite-serandite structure form discrete phases, as shown by the scattered grains of cerianite-(Ce), and thorium-bearing cerianite in association with the eudialyte and its alteration assemblages. Published thermodynamic data show that cerianite in most natural geological conditions is stable under neutral to alkaline conditions and in oxidizing conditions, i.e. at positive Eh values (Braun *et al.*, 1990; Akagi and Masuda, 1998; Pan and Stauffer, 2000). Moreover, experimental data show that *LREE*s are more mobile than *HREE*s in a chlorinated environment. Thus, during the peak alkalinity stage, the majority of the *LREE*s will remain in the hydrothermal fluid as shown by the relatively low concentrations of *LREE*s in the hydrothermal eudialyte (see table 2 of Mitchell and Chakrabarty, 2012), and any change of pH towards smaller values would definitely enhance the precipitation of *LREE*. Thus, formation of *REE*-rich accessory phases such as cerianite-(Ce) indicates a decrease in pH relative to the alkalinity prevailing during hydrothermal eudialyte formation. This conclusion is supported by the presence of Ce^{4+} (as CeO_2) in cerianite-(Ce) indicating an oxidizing environment.

In contrast to the agpaitic gneisses, the miaskitic gneisses of Sushina are characterized by the dominance of orthoclase over albite, nepheline along with sporadic occurrences of 'eastonitic'-ferroan phlogopite (Mitchell and Chakrabarty, 2012). These rocks lack completely typomorphic minerals of the agpaitic system and contain accessory zircon, titanite and magnetite;

minerals which are generally considered as characteristic of miaskitic nepheline syenites. Thus, hingganite-(Ce) found within the miaskitic syenite gneiss probably represents the superposition of an agpaitic typomorphic mineral on an initial miaskitic assemblage. Textural relationships suggest that the hingganite is commonly found to be replacing the magmatic zircons and thus considered as late in the paragenetic history compared to the common rock forming minerals such as feldspars and nepheline. Of the various *REE* phases occurring at Sushina, hingganite-(Ce) is the most Nd rich (13.9−15.40 wt.% Nd_2O_3). Available experimental data show that enrichment factors for the *LREE*s varies significantly between the temperature 400 and 200ºC (Williams-Jones *et al.*, 2012) compared to the *HREE*s. Among the *LREE*s, maximum Gd and Nd enrichment takes place at ~400 and 350ºC, respectively. In contrast, peak Ce and La enrichment takes place at much lower temperatures (~300ºC and ~200ºC, respectively). Minerals of the gadolinite–datolite group represented by hingganite-(Ce) are the most La- and Nd-rich phases found at Sushina and their crystallization temperature can be estimated in the range of 400−300ºC, followed by the cerianite-(Ce) at a lower temperature; probably <300ºC. The estimated crystallization temperature for cerianite-(Ce) and hingganite-(Ce), which were precipitated from the deuteric fluid, thus indicate that eudialyte decomposition was initiated at temperatures >400ºC. This is in agreement with the observed subsolidus alteration of eudialyte at the Pilansberg complex where subsolidus/deuteric alteration related to eudialyte is considered to have occurred at temperatures of <450ºC (Mitchell and Liferovich, 2006).

Conclusions

This work reports the occurrence of *REE* minerals from the Sushina Hill Complex. The most rare earth-rich assemblage is represented by rinkite, cerianite-(Ce) and hingganite-(Ce). The presence of these *REE*-rich phases indicates an overall agpaitic nature for peralkaline nepheline-syenite gneisses. These minerals indicate successive phases of crystallization from an early magmatic to post-magmatic/hydrothermal stages within a temperature range of 500−200ºC. Rinkite, was the first *REE*-rich mineral to crystallize from the parent melt and is of unusual composition, being the most Nd-rich rinkite reported to date. Rinkite is considered to be a primary agpaitic mineral and indicates an elevated Na/F ratio during the early stage of the crystallization history. Hydrothermally-formed cerianite-(Ce) found in association with the rinkite, eudialyte and its alteration assemblage is characterized by significant contents of Y and *REE*. Cerianite-(Ce) is the most Ce-rich phase found at Sushina and represents formation at relatively lower pH and lower temperature (<~300ºC) than the associated eudialytes and related alteration assemblages. In contrast to these phases hingganite-(Ce) is hosted by the miaskitic syenite gneiss and its presence indicates superposition of an agpaitic assemblage on the early-formed miaskitic assemblage. Thus, the miaskitic rocks are the oldest lithological unit of the complex. The hingganite-(Ce) is characterized by significant amounts of the *LREE* (La, Ce, Nd) and has a probable crystallization temperature in the range of 400−300ºC.

Acknowledgements

We thank the Head, Institute Instrumentation Centre (IIC), IIT Roorkee for use of the SEM-EDAX and EPMA facility at IIC. A grant from the UGC (University Grant Commission) provided to AC for financial support through a Minor Research Project (MRP) (No.F. PSW-009/11-12, SNO. 205847) is duly acknowledged. The research benefitted from helpful discussions with R.N. Chakrabarty, P. Samanta, S. Mukhopadhyay and A.C. Mahato. Constructive comments by two anonymous reviewers substantially improved the quality of the manuscript. The editorial care of Prof. Peter Williams and Dr W.A. Crichton is much appreciated.

References

Adamson, O.J. (1944) The petrology of the Norra Kärr district. *Geologiska Føreningen Stockholm Førhandlingar*, **66**, 113−255.

Akagi, T. and Masuda, A. (1998) A simple thermodynamic interpretation of Ce anomaly. *Geochemical Journal*, **32**, 301−314.

Allan, J.F. (1992) Geology and mineralization of the Kipawa Yttrium-Zirconium Prospect, Québec. *Exploration and Mining Geology*, **1**, 283−295.

Basu, S.K. (1993) Alkaline-Carbonatite Complex in Precambrian of South Purulia Shear Zone, Eastern India: Its characteristics and mineral potentialities, *Indian Minerals*, **47**, 179−194.

Belkin, H.E., Macdonald, R. and Grew, E.S. (2009) Chevkinite-group minerals from granulite-facies

metamorphic rocks and associated pegmatites of East Antarctica and South India. *Mineralogical Magazine*, **73**, 149–164.

Bhattacharya, H.N. and Bandyopadhaya, S. (1998) Seismites in a Proterozoic tidal succession, Singhbhum, Bihar, India. *Sedimentary Geology*, **119**, 239–252.

Blaxland, A.B. (1977) Agpaitic magmatism at Norra Kärr? Rb-Sr isotopic evidence. *Lithos*, **10**, 1–8.

Braun, J.-J., Pagel, M., Muller, J.-P., Bilong, P., Michard, A. and Guillet, B. (1990) Cerium anomalies in lateritic profiles. *Geochimica et Cosmochimica Acta*, **54**, 781–795.

Cámara, F., Sokolova, E. and Hawthorne, F.C. (2011) From structure topology to chemical composition. XII. Titanium silicates: the crystal chemistry of rinkite, $Na_2Ca_4REETi(Si_2O_7)_2OF_3$. *Mineralogical Magazine*, **75**, 2755–2774.

Chakrabarty, A. (2009) *Petrogenesis of carbonatite and associated alkaline rocks, Purulia, W.B., India*. Ph.D. Thesis, Department of Earth Sciences, Indian Institute of Technology Roorkee.

Chakrabarty, A., Mahato, A.C., Ren, M. and Sen, A.K. (2013) The Sushina Hill Peralkaline Complex, West Bengal, India: A Mineralogical Paradise. *18th Convention of Indian Geological Congress & International Symposium* "*Minerals and Mining in India – The way forward, inclusive of cooperative mineral-based industries in SAARC countries*" (extended Abstract), pp. 121–122.

Chakrabarty, A., Pruseth, K.L. and Sen, A.K. (2011) First report of eudialyte occurrence from the Sushina Hill Region, Purulia District, West Bengal. *Journal of the Geological Society of India*, **77**, 12–16.

Chakrabarty, A., Pruseth, K.L. and Sen, A.K. (2012) Composition and petrogenetic significance of the eudialyte group of minerals from Sushina, Purulia, West Bengal. *Journal of the Geological Society of India*, **79**, 449–459.

Chakrabarty, A., Sen, A.K. and Ghosh, T.K. (2009) Amphibole – A key indicator mineral for petrogenesis of carbonatite from Purulia, West Bengal, India. *Mineralogy and Petrology*, **95**, 105–112.

Chakrabarty, A. and Sen, A.K. (2010) Enigmatic association of the carbonatite and alkali-pyroxenite along the Northern Shear Zone: A saga of primary magmatic carbonatites. *Journal of the Geological Society of India*, **74**, 403–413.

Chakrabarty, A. and Sen, A.K. (2013) Geochronological constraints and tectonic implications of the alkaline rocks of South Purulia Shear Zone, W.B., India. *18th Convention of Indian Geological Congress & International Symposium* "*Minerals and Mining in India-The way forward, inclusive of cooperative mineral-based industries in SAARC countries*" (extended Abstract), pp 86–88.

Chatterjee, N., Crowley, J.L. and Ghose, N.C. (2008) Geochronology of the 1.55 Ga Bengal anorthosite and Grenvillian metamorphism in the Chotanagpur gneissic complex, eastern India. *Precambrian Research*, **161**, 303–316.

Chatterjee, N., Banerjee, M., Bhattacharya, A. and Maji, A.K. (2010) Monazite chronology, metamorphism–anatexis and tectonic relevance of the mid-Neoproterozoic Eastern Indian Tectonic Zone. *Precambrian Research*, **179**, 99–120.

Chatterjee, N. and Ghose, N.C. (2011) Extensive Early Neoproterozoic high-grade metamorphism in North Chotanagpur Gneissic Complex of the Central Indian Tectonic Zone. *Gondwana Research*, **20**, 362–379.

Curtis, L.W. and Currie, K.L. (1977) Geology and petrology of the Red Wine complex, central Labrador. *Geological Survey of Canada Bulletin*, **287**, 61.

Demartin, F., Pilati, T., Diella, V., Gentile, P. and Gramaccioli, C.M. (1993) A crystal-chemical investigation of Alpine gadolinite. *The Canadian Mineralogist*, **31**, 127–136.

Demartin, F., Minaglia, A. and Gramaccioli, C.M. (2001) Characterization of gadolinite-group minerals using crystallographic data only: the case of hingganite-(Y) from Cuasso Al Monte, Italy. *The Canadian Mineralogist*, **39**, 1105–1114.

Edgar, A.D. and Blackburn, C.E. (1972) Eudialyte from the Kipawa Lake area, Temiscamingue County, Québec. *The Canadian Mineralogist*, **11**, 554–559.

Eriksson, P.G., Mazumder, R., Catuneanu, O., Bumby, A.J. and Ilondo, B.O. (2006) Precambrian continental freeboard and geological evolution: A time perspective. *Earth-Science Reviews*, **79**, 165–204.

Frondel, C. and Marvin, U.B. (1959) Cerianite, CeO_2, from Poços de Caldas, Brazil. *American Mineralogist*, **44**, 882–884.

Goswami, J.N., Mishra, S., Wiedenbeck, M., Ray, S.L. and Saha, A.K. (1995) 3.55 Ga old zircon from Singhbhum-Orissa iron ore Craton, Eastern India. *Current Science*, **69**, 1008–1011.

Goswami, B. and Basu, S.K. (2013) Metamorphism of Proterozoic agpaitic nepheline syenite gneiss from North Singhbhum Mobile Belt, eastern India. *Mineralogy and Petrology*, **107**, 517–538.

Graham, A.R. (1955) Cerianite CeO_2: a new rare-earth oxide mineral. *American Mineralogist*, **40**, 560–564.

Grew, E.S. (2002) Mineralogy, petrology and geochemistry of Beryllium: An introduction to and list of Beryllium minerals. Pp. 1–76 in: *Beryllium – Mineralogy – Petrology and Geochemistry* (E.S. Grew, editor). Reviews in Mineralogy and Geochemistry, **50**. Mineralogical Society of America and the Geochemical Society, Washington, D.C.

Guastoni, A., Nestola, F. and Giaretta, A. (2009)

Mineral chemistry and alteration of rare earth element (REE) carbonates from alkaline pegmatites of Mount Malosa, Malawi. *American Mineralogist*, **94**, 1216–1222.

Holtstam, D. and Andersson, U.B. (2007) The REE minerals of the Bastnäs-type deposits, south-central Sweden. *The Canadian Mineralogist*, **45**, 1073–1114.

Ito, J. and Hafner, S.S. (1974) Synthesis and study of gadolinites. *American Mineralogist*, **59**, 700–708.

Jambor, J.L., Roberts, A.C., Grice, J.D., Birkett, T.C., Gorat, L.A. and Zajac, S. (1998) Gernite-(Y), $(Ca,Na)_2(Y,REE)_3Si_6O_{18}.2H_2O$, a new mineral species, and an associated Y-bearing gadolinite-group mineral, from the Strange Lake Peralkaline Complex, Quebec-Labrador. *The Canadian Mineralogist*, **36**, 793–800.

Lorenzen, J. (1884) Untersuchung einiger Mineralienaus Kangerdluarsuk in Grönland. *Zeitschrift für Kristallographie*, **9**, 243–254.

Lottermoser, B.G. (1987) Churchite from the Mt Weld carbonatite laterite, Western Australia. *Mineralogical Magazine*, **51**, 468–469.

Maji, A.K., Goon, S., Bhattacharya, A., Mishra, B., Mahato, S. and Bernhardt, H.J. (2008) Proterozoic polyphase metamorphism in the Chhotanagpur Gneissic Complex (India), and implication for trans-continental Gondwanaland correlation. *Precambrian Research*, **162**, 385–402.

Markl, G. and Baumgartner, L. (2002) pH changes in peralkaline late-magmatic fluids. *Contributions to Mineralogy and Petrology*, **144**, 331–346.

Marks, M.A.W., Hettmann, K., Schilling, J., Frost, B.R. and Markl, G. (2011) The mineralogical diversity of alkaline igneous rocks: critical factors for the transition from miaskitic to agpaitic phase assemblages. *Journal of Petrology*, **52**, 439–455.

Matsumoto, Y. and Sakamoto, A. (1982) Preliminary report on metamict cerianite from Nesöya, Lützow-Holmbukta, East Antarctica. *Memoirs of National Institute of Polar Research*, **21**, 103–111.

Mazumder, R. (2005) Proterozoic sedimentation and volcanism in the Singhbhum crustal province, India and their implications, *Sedimentary Geology*, **176**, 167–193.

Mishra, S., Deomurari, M.P., Widenbeck, M., Goswami, J.N., Ray, S.L. and Saha, A.K. (1999) $^{207}Pb/^{206}Pb$ zircon ages and the evolution of the Singhbhum craton, eastern India: an ion microprobe study. *Precambrian Research*, **93**, 139–151.

Mitchell, R.H. and Chakrabarty, A. (2012) Paragenesis and decomposition assemblage of a Mn-rich eudialyte from the Sushina peralkaline nepheline syenite gneiss, Paschim Banga, India. *Lithos*, **152**, 218–226.

Mitchell, R.H. and Liferovich, R.P. (2006) Subsolidus deuteric/hydrothermal alteration of eudialyte in lujavrite from the Pilansberg alkaline complex, South Africa. *Lithos*, **91**, 352–372.

Miyawaki, R., Nakai, I. and Nagashima, K. (1984) A refinement of the crystal structure of gadolinite. *American Mineralogist*, **69**, 948–953.

Miyawaki, R., Matsubara, S., Yokoyama, K. and Okamoto, A. (2007) Hingganite-(Ce) and hingganite-(Y) from Tahara, Hirukawa-mura, Gifu Prefecture, Japan: The description on a new mineral species of the Ce-analogue of hingganite-(Y) with a refinement of the crystal structure of hingganite-(Y). *Journal of Mineralogical and Petrological Sciences*, **102**, 1–7.

Pan, Y. and Stauffer, M.R. (2000) Cerium anomaly and Th/U fractionation in the 1.85 Ga Flin Flon Paleosol: clues from *REE*- and U-rich accessory minerals and implications for paleoatmospheric reconstruction. *American Mineralogist*, **85**, 898–911.

Papoutsa, AD. and Pe-Piper, G. (2013) The relationship between REE-Y-Nb-Th minerals and the evolution of an A-type granite, Wentworth Pluton, Nova Scotia. *American Mineralogist*, **98**, 444–462.

Pearson, R.G. (1963) Hard and soft acids and bases. *Journal of the American Chemical Society*, **85**, 3533–3539.

Pezzotta, F., Diella, V. and Guastoni, A. (1999) Chemical and paragenetic data on gadolinite-group minerals from Baveno and Cuasso al Monte, southern Alps, Italy. *American Mineralogist*, **84**, 782–789.

Pfaff, K., Krumrei, K., Marks, M., Wenzel, T., Rudolf, T. and Markl, G. (2008) Chemical and physical evolution of the 'lower layered sequence' from the nepheline syenitic Ilímaussaq intrusion, South Greenland: Implications for the origin of magmatic layering in peralkaline felsic liquids. *Lithos*, **106**, 280–296.

Pouchou, J.L. and Pichoir, F. (1991) Quantitative analysis of homogeneous or stratified microvolumes applying the model "PAP". Pp 31–75 in: *Electron Probe Quantitation* (K.F.J. Heinrich and D.E. Newbury, editors). Plenum Press, New York.

Pršek, J., Ondrejka, M., Bačík, P., Budzy and Uher, P. (2010) Metamorphic-hydrothermal REE minerals in the Bacúch magnetite deposit, Western Carpathians, Slovakia: (Sr, S)-rich monazite-(Ce) and Nd-dominant hingganite. *The Canadian Mineralogist*, **48**, 81–94.

Rekha, S., Upadhyay, D., Bhattacharya, A., Kooijman, E., Goon, S., Mahato, S. and Pant, N.C. (2011) Lithostructural and chronological constraints for tectonic restoration of Proterozoic accretion in the Eastern Indian Precambrian shield. *Precambrian Research*, **187**, 313–333.

Saha, A.K. (1994) Crustal evolution of Singhbhum-

North Orissa, Eastern India. *Memoir of the Geological Society of India*, **27**, 341.

Sanyal, S. and Sengupta, P. (2012) Metamorphic evolution of the Chotanagpur Granite Gneiss Complex of East Indian Shield: current status. Pp. 117–145 in: *Palaeoproterozoic of India* (R. Mazumder and D. Saha, editors). Special Publications, **365**. Geological Society, London.

Schilling, J., Wu, F.-Y., McCammon, C., Wenzel, T., Marks, M.A.W., Pfaff, K., Jacob, D.E. and Markl, G. (2011) The compositional variability of eudialyte-group minerals. *Mineralogical Magazine*, **75**, 87–115.

Segalstad, T.M. and Larsen, A.O. (1978) Gadolinite-(Ce) from Skien, southwestern Oslo region, Norway. *American Mineralogist*, **63**, 188–195.

Skublov, S.G., Astaf'ev, B.Yu., Marin, Yu.B., Gembitskaya, I.M. and Levchenkov, O.A. (2009) First find of cerianite in zircons from metasomatites of the Terskii Greenstone Belt, Baltic Shield. *Doklady Earth Sciences*, **428**, 1134–1138.

Sørensen, H. (1992) Agpaitic nepheline syenites: a potential source of rare elements. *Applied Geochemistry*, **7**, 417–427.

Sørensen, H. (1997) The agpaitic rocks – an overview. *Mineralogical Magazine*, **61**, 485–498.

Styles, M.T. and Young, B.R. (1983) Fluocerite and its alteration products from the Afu Hills, Nigeria. *Mineralogical Magazine*, **47**, 41–46.

Van Wambeke, L. (1977) The Karonge rare earth deposits, Republic of Burundi: new mineralogical-geochemical data and origin of the mineralization. *Mineralium Deposita*, **12**, 373–380.

Williams-Jones, A.E., Migdisov, A.A. and Samson, I.M. (2012) Hydrothermal mobilisation of the Rare Earth Elements – a Tale of "Ceria" and "Yttria". *Elements*, **8**, 355–360.

Zaitsev, A.N., Chakhmouradian, A.R., Sidra, O.I., Spratt, J., Williams, C.T., Stanley, C.J., Petrov, S.V., Britvin, S.N. and Polyakova, E.A. (2011) Fluorine-, yttrium- and lanthanide-rich cerianite-(Ce) from carbonatitic rocks of the Kerimasi volcano and surrounding explosion craters, Gregory Rift, northern Tanzania. *Mineralogical Magazine*, **75**, 2813–2822.